

SIMULATION STUDY OF LASER WAKEFIELD ACCELERATION VARYING THE DOWN-RAMP LENGTH OF A GAS JET

R. P. Nunes*, UFRGS, Porto Alegre, Brasil
A. Bonatto, UFSCPA, Porto Alegre, Brasil
E. P. Maldonado, ITA, São José dos Campos, Brasil
R. E. Samad, N. D. Vieira Jr, IPEN-CNEN, São Paulo, Brasil

Abstract

In this work, particle-in-cell simulations were carried out to investigate the role of the down-ramp length of a H_2 gas jet in accelerating electrons ionized by the laser pulse. The laser and plasma density were chosen so that the system is operating in the self-modulated regime. Preliminary results show how the down-ramp length can control the injection of electrons in the first bubble induced in the plasma by the laser pulse.

INTRODUCTION

The conventional method of accelerating charged particles is by generating electric fields. Traditionally, the accelerating electric fields have been produced by radio-frequency generators. More recently, plasmas have been proposed as transformer media for producing high-amplitude electric fields in short distances [1]. With this technique, through a laser pulse or a beam, a wakefield is produced in the plasma, which can accelerate charged particles with gradients of GV/cm [2, 3]. This plasma-based technique might allow for high-energy compact accelerators to become available for a wide variety of applications.

Besides overall compactness, many applications might require accelerators operating at high frequencies. For this purpose, the use of gas jets produced by nozzles as targets, which are ionized by the laser pulse, generating the plasma medium for acceleration, become an interesting alternative.

The purpose of this work is to provide a brief investigation on the effect of the down-ramp length of a trapezoidal-shape gas jet with the aid of particle-in-cell simulations. The next section presents the results and a brief discussion with preliminary conclusions.

SIMULATION AND DISCUSSIONS

In this work, a gaussian laser pulse, with waist $w_0 = 7 \mu\text{m}$, and longitudinal extension $c\tau = 15 \mu\text{m}$, propagates along a gas jet with a trapezoidal longitudinal density profile, which has an up ramp with length $80 \mu\text{m}$, a plateau of $40 \mu\text{m}$, and a down ramp, which is varied from $20 \mu\text{m}$ to $140 \mu\text{m}$, in steps of $20 \mu\text{m}$. The gas jet density in the plateau is $n_0 \approx 2 \times 10^{20} \text{ atoms/cm}^3$, and the laser is focused at the middle of the up ramp. The laser pulse ionizes the gas, driving a wakefield, and hence being self-modulated, resulting in acceleration of plasma electrons. Since the $80 \mu\text{m}$ down-ramp length case is discussed in another IPAC'21

proceeding [4], it is not presented here. The simulations were carried out by using the FBPIC code [5]. Simulation properties are also described in the previously mentioned reference.

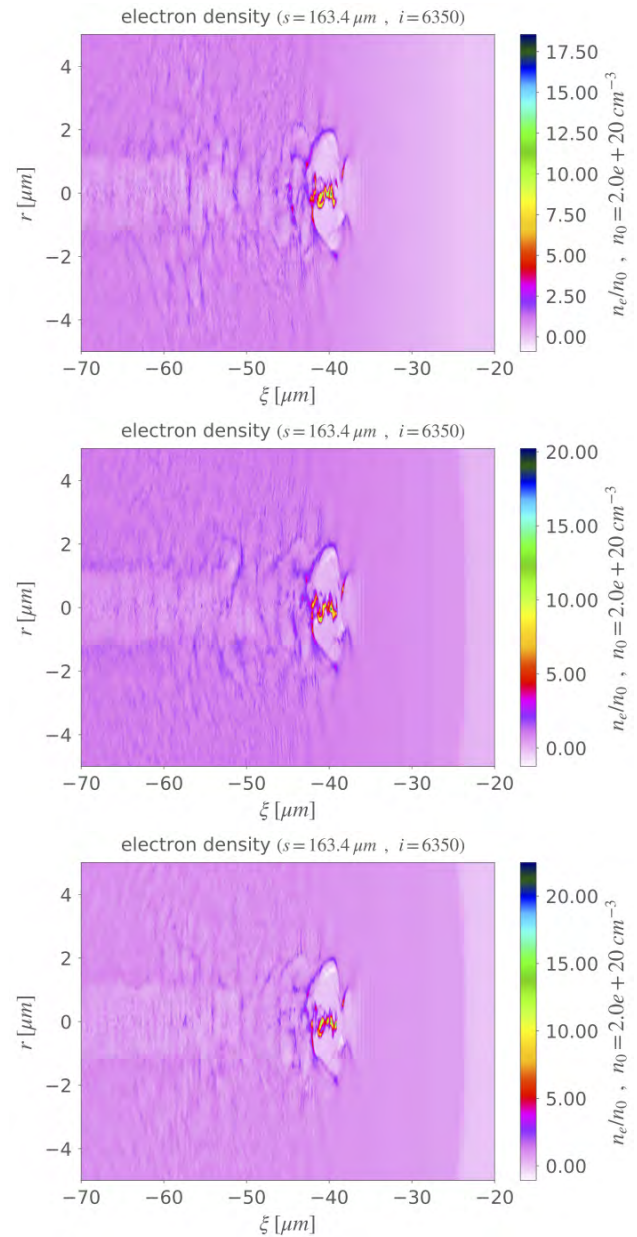


Figure 1: Electron-plasma density for down-ramp lengths of $20 \mu\text{m}$, $40 \mu\text{m}$, and $60 \mu\text{m}$.

* roger.pizzato@ufrgs.br

Figure 1 presents the electron-plasma density for the down-ramp lengths of 20 μm , 40 μm , and 60 μm , while in Fig. 2 the same is shown for 100 μm , 120 μm , and 140 μm . $\xi = z - s$ is the co-moving coordinate, z is the longitudinal coordinate, and s is the propagated distance. Note that, for the same propagated distance $s = 163.4 \mu\text{m}$, the density of plasma electrons is mostly the same in shape and in intensity. There are two bubbles (rounded light-pink regions), the first incomplete, followed by a well-defined second bubble. While the first bubble is empty, there are electrons inside the second one, demonstrating that injection has occurred earlier in simulation.

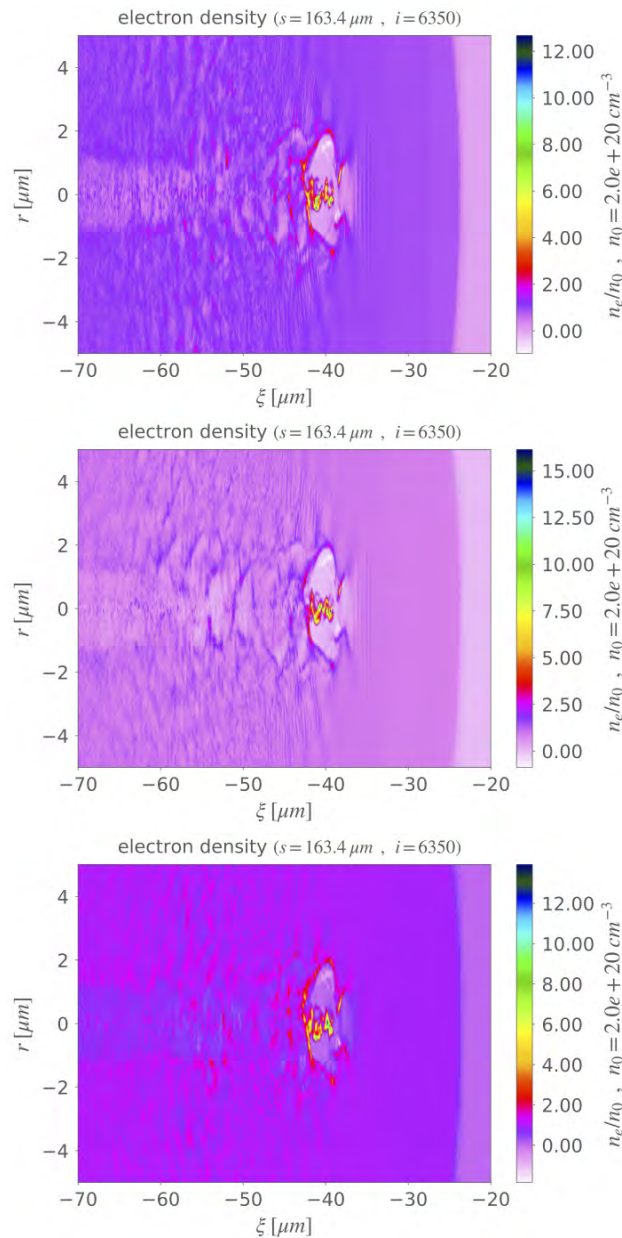


Figure 2: Electron-plasma density for down-ramp lengths of 100 μm , 120 μm , and 140 μm .

Figure 3 shows again the density of plasma electrons for down-ramp lengths of 100 μm , 120 μm , and 140 μm . Now, a longer propagated distance is considered, $s \approx 190 \mu\text{m}$. It can be seen that the first bubble shown in Fig. 2 is now completed. Moreover, there are now electrons inside this first bubble, indicating that the electrons previously injected in the second bubble have been accelerated enough to be injected in the first bubble. This electron injection in the first bubble has not been observed for the down-ramp lengths of 20 μm , 40 μm , and 60 μm cases.

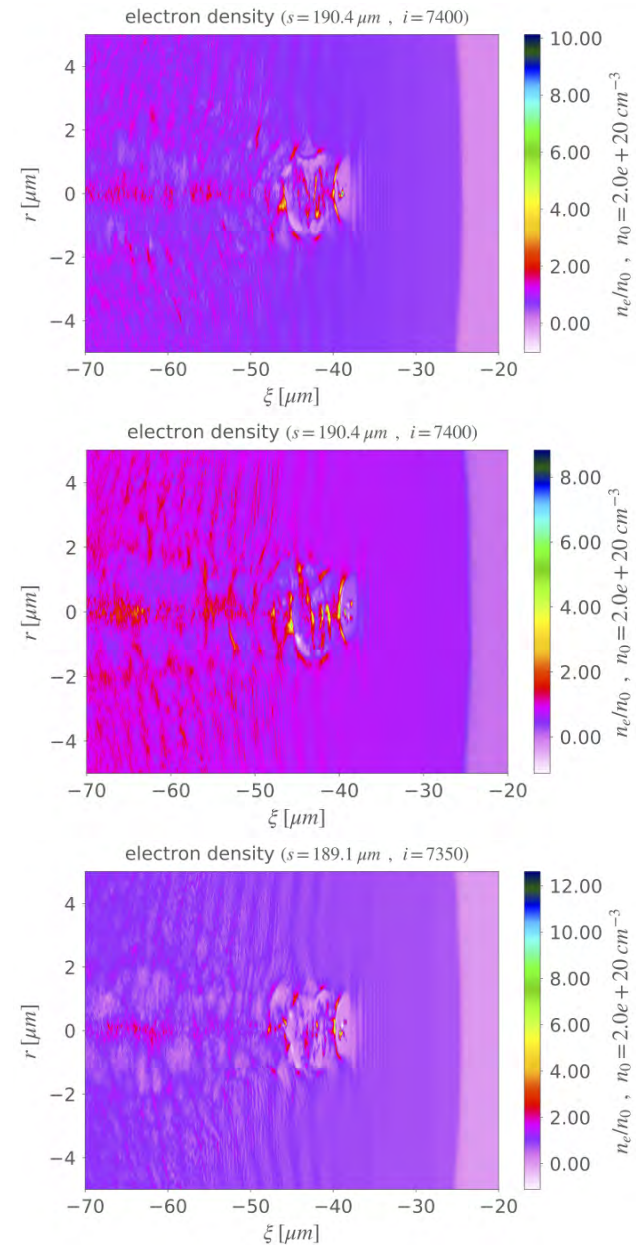


Figure 3: Electron-plasma density for down-ramp lengths of 100 μm , 120 μm , and 140 μm .

Figure 4 presents the accelerated bunches exiting the gas jet for 20 μm , 40 μm , and 60 μm down-ramp lengths. See that the bunches are a diffuse cloud of electrons, resulting from the acceleration in the second bubble over the whole gas jet length. Figure 5 shows the bunches produced by down-ramp lengths of 100 μm , 120 μm , and 140 μm . It is possible to see that, besides the diffuse cloud already seen for the other cases, there is now also the presence of a leading bunch, which is a result from injection in the first bubble.

From this brief analysis, it can be perceived that the down-ramp length of the gas jet can be used to control electron injection. As shown here, while injection has occurred only in the second bubble for the down-ramp lengths of 20 μm ,

40 μm , and 60 μm cases, for the 100 μm , 120 μm , and 140 μm cases injection has occurred in the first bubble. The visual difference observed in the accelerated electrons is the presence of a leading bunch for the down-ramp lengths of 100 μm , 120 μm , and 140 μm cases. Future works will address the quantitative analysis of the accelerated electrons shown here.

ACKNOWLEDGEMENTS

The authors acknowledge the computational support provided by Laboratório Nacional de Computação científica (LNCC), in which the PIC simulations were carried out.

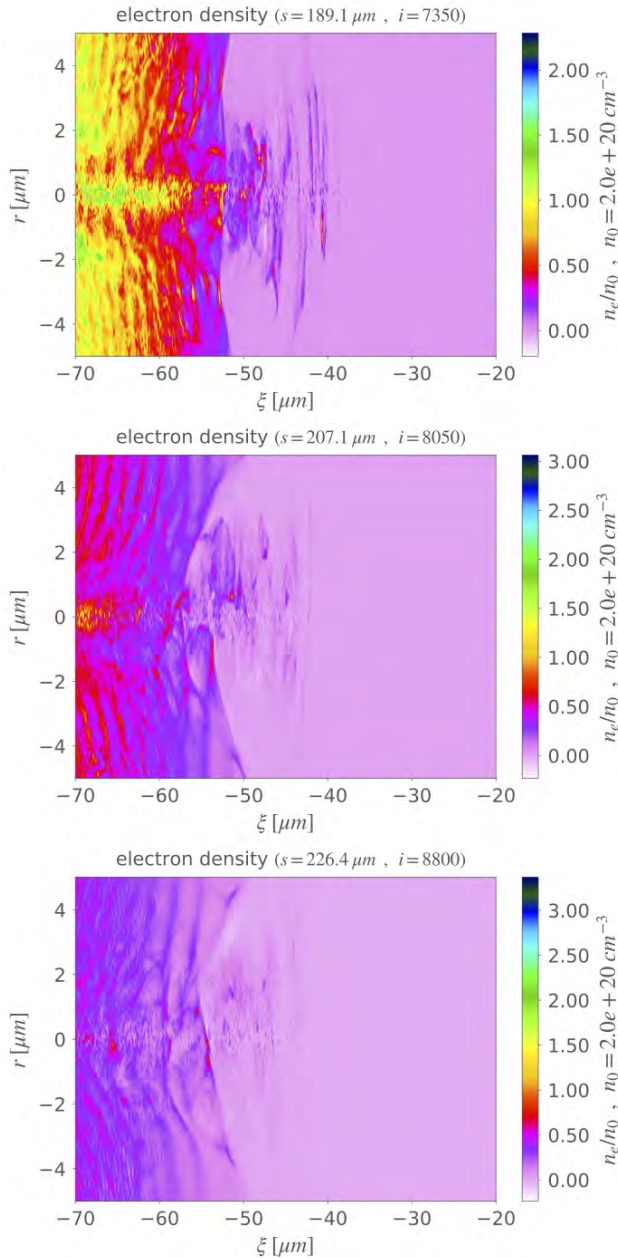


Figure 4: Accelerated bunches for down-ramp lengths of 20 μm , 40 μm , and 60 μm .

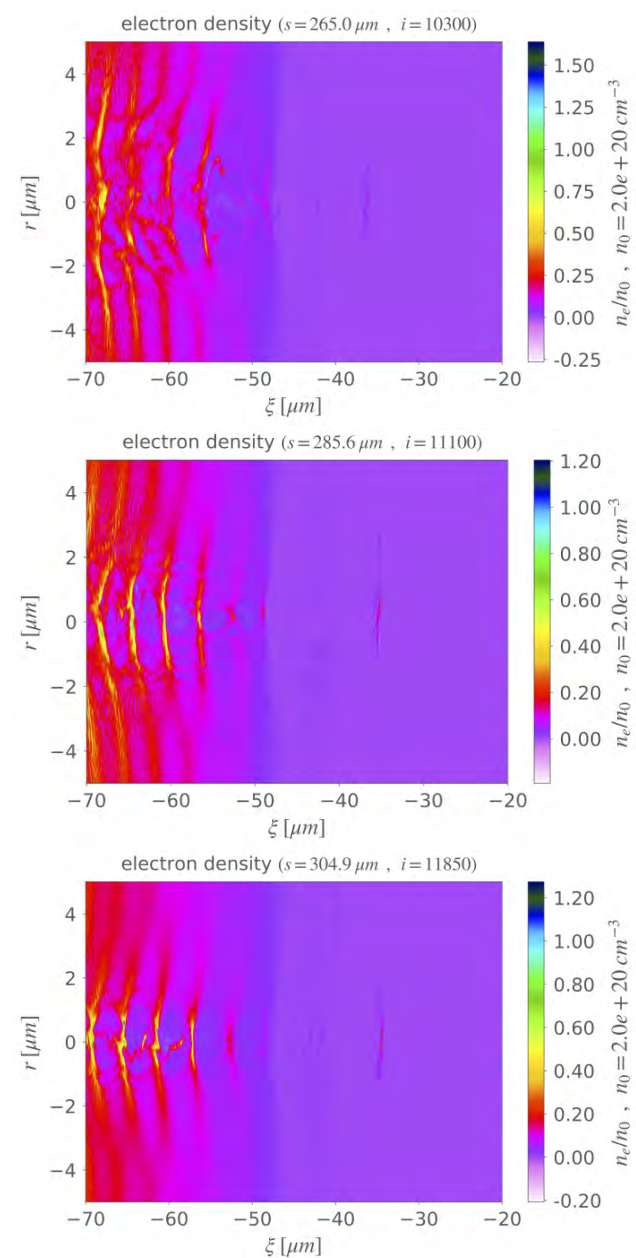


Figure 5: Accelerated bunches for down-ramp lengths of 100 μm , 120 μm , and 140 μm .

REFERENCES

- [1] T. Tajima and J. M. Dawson, "Laser Electron Accelerator", *Phys. Rev. Lett.*, vol. 43, no. 4, pp. 267-270, Jul. 1979.
- [2] E. Esarey, P. Sprangle, J. Krall, and A. Ting, "Overview of plasma-based accelerator concepts", *IEEE Trans. Plasma Sci.*, vol. 24, no. 2, pp. 252-288, Apr. 1996.
doi:10.1109/27.509991
- [3] E. Esarey, C. B. Schroeder, and W. P. Leemans, "Physics of laser-driven plasma-based electron accelerators", *Rev. Mod. Phys.*, vol. 81, no. 3, pp. 1229-1285, Aug. 2009.
doi:10.1103/revmodphys.81.1229
- [4] R.P. Nunes, A. Bonatto, E. P. Maldonado, R. E. Samad, and N. V. Dias Jr, "Laser Pulse Dynamics in the Self-Modulated Regime", presented at the 12th Int. Particle Accelerator Conf. (IPAC'21), Campinas, Brazil, May 2021, paper TUPAB143.
- [5] R. Lehe, M. Kirchen, I. A. Andriyash, B. B. Godfrey, and J. Vay, "A spectral, quasi-cylindrical and dispersion-free Particle-In-Cell algorithm", *Comput. Phys. Commun.*, vol. 203, pp. 66-82, June 2016. doi:10.1016/j.cpc.2016.02.007